Paleomagnetic and geochronological identification of the R6union subchron in Ethiopian Afar

Tesfaye Kidane, X Quidelleur, J Carlut, V Courtillot, Y. Gallet, P.Y. Gillot, Tigistu Haile

JOURNAL OF GEOPHYSICAL RESEARCH, VOL. 104, NO. B5, PAGES 10,405–10,419, MAY 10, 1999

Paleomagnetic and geochronological identification of the Réunion subchron in Ethiopian Afar

Tesfaye Kidane,[1,3] J. Carlut,[1] V. Courtillot,[1] Y. Gallet,[1]
X. Quidelleur,[1,2] P.Y. Gillot,[2] and Tigistu Haile[3]

Abstract. This paper reports the paleomagnetic and geochronological analysis of a suite of samples from a basaltic fault-related scarp of Pliocene age in the central part of the Afar depression (Ethiopia). Paleomagnetic work uncovers a clear characteristic remanent magnetization carried by (titano-) magnetites, with high unblocking temperatures, close to the Curie temperature of pure magnetite. The characteristic direction, based on 27 non transitional flows, is D=8.1°, I=10.1° (α_{95}=4.1°). This is consistent with earlier determinations of the clockwise tectonic rotation, due to rift propagation and overlap, of the block to which the section belongs. Magnetic stratigraphy consists of a succession from bottom to top of 16 reversed, 7 normal, and 4 reversed flows. One flow at the upper normal to reverse transition demonstrates complex behavior upon thermal and alternating field (AF) demagnetization, which is due to remagnetization by the overlying flow. K/Ar dating of five samples provides consistent determinations, averaging 2.07 ± 0.05 Ma. All ages agree with this average, given their rather large individual uncertainties (from 0.04 to 0.08 Ma at the 1σ level). Comparison with recent reference geomagnetic polarity timescales (GPTS) indicates that the normal subchron recorded in the Gamarri section must be linked with (one of) the Réunion event(s). The normal subchron and an earlier episode of large secular variation could provide the best volcanic record of a double Réunion event. Although uncertainties in ages are too large to allow unequivocal inferences, our age determination for the Réunion event is in better agreement with earlier determinations of *McDougall and Watkins* [1973] than with a more recent value proposed by *Baksi et al.* [1993] and used in the GPTS.

1. Introduction

The Afar triangle lies at the triple junction of the Red Sea, Gulf of Aden, and Ethiopian rifts. The floor of the triangular depression is mostly covered by young lava, most prominently by the widespread so-called stratoid basalts [*Varet*, 1975]. These basalts were severely faulted as the Gulf of Aden and Red Sea rifts propagated toward each other [*Courtillot*, 1980, 1982] and now form an active overlap [*Tapponnier et al.*, 1990; *Manighetti*, 1993; *Manighetti et al.*, 1997]. Acquisition of paleomagnetic and geochronologic data has been a key to understanding the tectonics of the area. *Courtillot et al.* [1984] suggested that much of the trap-like stratoid series had been emplaced relatively fast between 1.3 and 2.2 Ma and demonstrated important block rotations of some 10° to 15°. This work was much extended by *Manighetti* [1993].

Therefore, up to now, the magnetic properties of Afar basalts have mostly been used for tectonic analysis. Yet they can also be very valuable for the study of the time and space characteristics of the geomagnetic field itself. On the basis of recent updated compilations of paleomagnetic data from lavas over the last 5 Myr [*Quidelleur et al.*, 1994; *Johnson and Constable*, 1996], the characteristics of the mean geomagnetic field are beginning to emerge [*McFadden et al.*, 1988; *Quidelleur et al.*, 1994; *Quidelleur and Courtillot*, 1996; *Johnson and Constable*, 1995, 1996; *Carlut and Courtillot*, 1998; *McElhinny et al.*, 1996]. Yet all these studies point out the need for better coverage both in space and time, and better quality data providing a full analysis of sampling, field, and laboratory uncertainties [*Carlut and Courtillot*, 1998]. There is also active interest in precisely describing the sequence of recent magnetic field reversals, with particular emphasis on accurate age determinations of key reversals and detailed analysis of very short chrons [e.g., *Valet and Meynadier*, 1993].

Recent active tectonics in Afar have exposed thick sequences of lava flows along high cliffs generated by normal faulting, providing exceptionally fresh series of great potential for magnetostratigraphic analysis. Unfortunately, many of these fault scarps are rather inaccessible, and parts were not even open to access until recently. We were able to sample in detail a series of 33 successive flows in 1995, along the Gamarri cliff, near the Afar capital of Aysaita, slightly west of the Djibouti-Ethiopian border (Figure 1). We report here the paleomagnetic and K/Ar geochronologic analyses of these lava flows, which apparently provide the second (and possibly best) volcanic record of the Réunion event and also have interesting consequences in terms of lava extrusion rate, rates of normal faulting, paleosecular variation of the geomagnetic field, and local tectonic rotations.

[1]Laboratoire de Paléomagnétisme et Géodynamique, Institut de Physique du Globe de Paris, Paris France.
[2]Laboratoire de Géochronologie, Université Paris-Sud, Orsay, France.
[3]Department of Geology and Geophysics, Addis Abba University, Addis Ababa, Ethiopia.

Paper number 1999JB900014.
0148-0227/99/1999JB900014$09.00

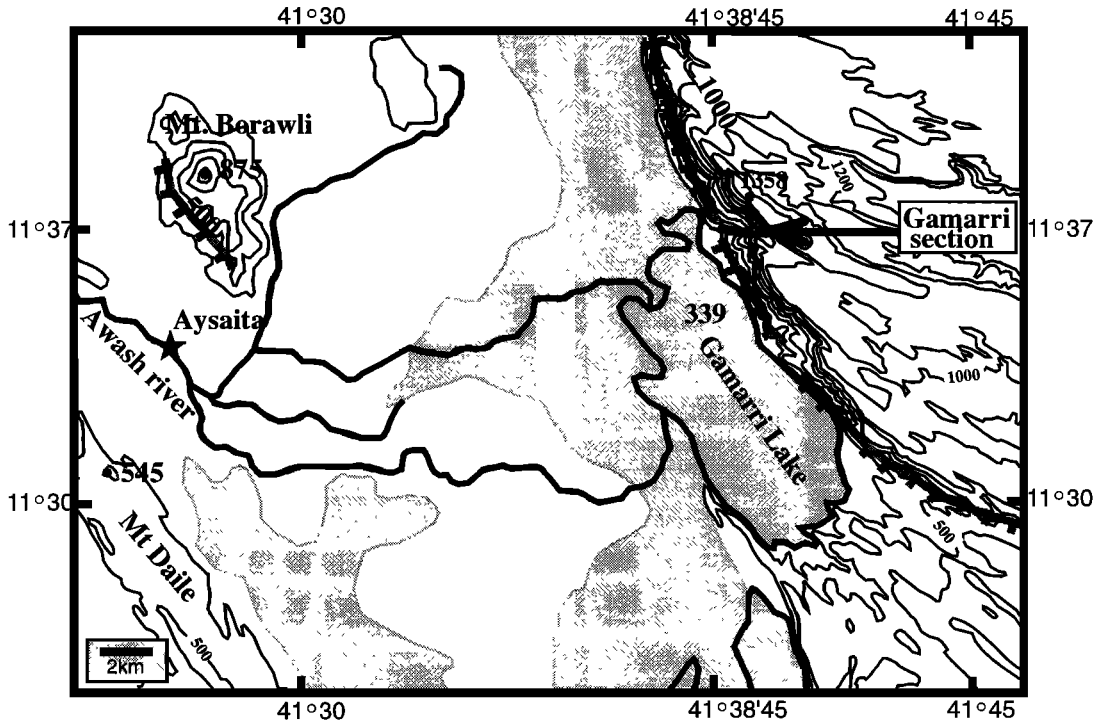

Figure 1. General location map of the Gamarri section in the central Afar depression (Ethiopia). Topographic altitudes (in m), contours (every 100 m), and main normal faults (rake symbol) are shown. Marshy areas are stippled.

2. Sampling

The Gamarri cliff was selected on the basis of a detailed search on Spot images, 1/250,000 topographic maps, and field exploration. The faulted western edge of the Gamarri block (Figure 1) [*Varet*, 1975; *Manighetti*, 1993] provided the least difficult access. The section is located along the marshy Gamarri Lake, formed as the Awash River abutts the upfaulted basalts and is deflected to the south. The main cliff consists of more than 100 lava flows exposed along a steep scarp, approximately 1500 m high. A small downfaulted block with an incised erosional channel and resulting alluvial fan provided access for sampling of successive flows from the base up to where the cliff became too steep to sample. Each flow was considered as a site and numbered upward, starting from GA01 up to GA22. At this point it was noted in the field that a small normal fault separated the lower section from the upper flows. On the basis of field inspection, the first flow above GA22 was thought to correspond to GA21 and was labeled GB11. In the same way, GB12 corresponded to GA22. Sampling had to be discontinued for safety reasons after reaching flow GB23. Altogether, 35 flows were sampled, but only 33 were actually distinct, as confirmed by later paleomagnetic analysis (below). Six to 10 cores of standard 2.5 cm diameter were drilled from each lava flow, providing a total of 261 cores for paleomagnetic analysis. All cores were oriented in the field both with solar and magnetic compasses. The mean difference between the two readings is 1.3°± 3.3°, in excellent agreement with earlier determinations in Afar (1.3° ± 2.6° and 1.2 ± 2.8° for two independent series of cores covering much of the Djibouti Republic [*Courtillot et al.*, 1984]) and also with the declination predicted from the 1995 International Geomagnetic Reference Field (IGRF) for the region (1.3°, with a secular rate of increase of 0.2°/yr). This indicates that local magnetic anomalies due to the basalts themselves are moderate and average out in the mean. In any case, use of solar azimuths minimizes errors in declination due to local magnetic anomalies. Careful inspection in the field led to the sampling of six of the very freshest flows for K/Ar dating. All of the monoclinal Gamarri lavas are slightly tilted in a uniform way by 5°, dipping to the east.

3. Paleomagnetic Experiments

3.1. Laboratory Treatment and Data Analysis

The cores were cut in the laboratory into 2.2 cm long specimens. Many cores allowed two, sometimes three companion specimens. Labeling was done in a systematic fashion for each core from base to top (closer to the exposed surface in the field). A total of 464 specimens were obtained; 375 were analyzed and led to the results presented here, the rest being available for further studies. All measurements were performed in the shielded room of the Institut de Physique du Globe de Paris (IPGP) paleomagnetic laboratory. Magnetic measurements were performed with a 2G cryogenic magnetometer (horizontal access, with three-coil online alternating field (AF) demagnetization with maximum peak field of 100 mT) and a JR5 spinner magnetometer. AF demagnetization was also done with a single-coil Schönstedt system. Thermal demagnetization was performed in two Pyrox, near-zero-field furnaces. As often as possible, twin specimens from the same core were subjected to both thermal (TH) and

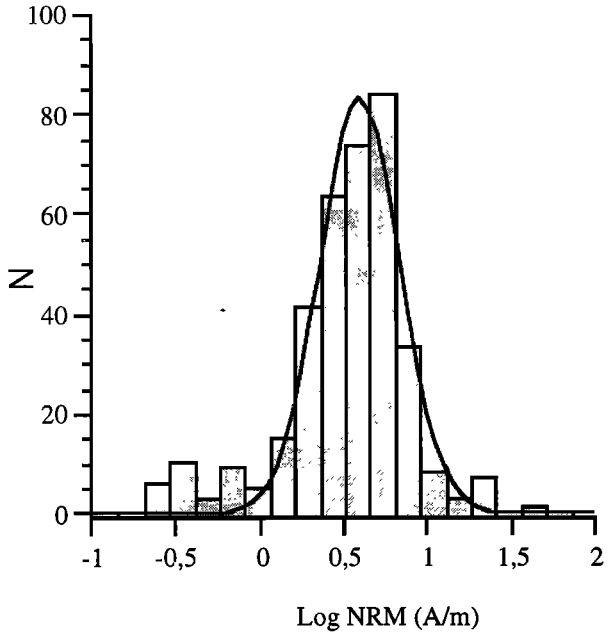

Figure 2. Histogram of natural remanent magnetization (NRM) intensities for 374 specimens. Best fitting log-normal curve is also shown (mean: 4.7 A/m).

alternating field (AF) demagnetizations, with 12 to 16 steps, in general.

Results of these demagnetizations were displayed graphically in the usual way as vector diagrams and components were determined by least squares analysis [*Kirshvink*, 1980]. Whenever stable endpoints and linear segments could not be isolated, because of overlap of several components, the technique of remagnetization circles was used [*Halls*, 1976, 1978]. Sample, site, and block averages were all determined using *Fisher* [1953] statistics or *McFadden and McElhinny* [1988] statistics for combined analysis of remagnetization circles and stable linear segments. A new comprehensive paleomagnetic software package by J.P. Cogné (personal communication, 1997) was used throughout to analyze all the data (from principal component analysis to overall mean directions). Strong field thermomagnetic and Curie balance experiments were performed for better identification of magnetic carriers in our Saint-Maur and Orsay facilities.

3.2. Natural Remanent Magnetization

The natural remanent magnetizations (NRMs) of the 375 analyzed specimens form a slightly skewed unimodal log normal distribution (Figure 2). If one excludes a single outlier with a magnetization of 330 A/m, which probably suffered lightning, the mean value is 4.7 A/m (95% confidence interval from 2.9 to 6.5 A/m), which compares favorably with the value found by *Prévot and Grommé* [1975] for continental and subaerial basalts (3.1-4.1 A/m). It also compares well with the values found in Afar by *Courtillot et al.* [1984], *Gruszow* [1992], and *Manighetti* [1993] for the stratoid basalts, which are of the order of 3.5 A/m (95% confidence interval from 1.7 to 7.4). NRM directions are scattered but clearly indicate two antipodal groups with declinations close to 180° and 360° and shallow inclinations, as expected.

3.3. Demagnetization

One hundred sixty-three specimens were demagnetized by AF in the 2G magnetometer, and 92 were demagnetized using the JR5 and Schönstedt demagnetizer. One hundred twenty specimens were thermally demagnetized. Sixty-nine specimens in each set were from twins of the same core. Representative results are illustrated as vector diagrams in Figure 3. In many cases, a low-coercivity component was removed by 10 mT, and a low unblocking temperature one was removed by 120° to 200°C. Though very scattered over an entire hemisphere, these components average quite precisely in the direction of the present field in Gamarri and are clearly dominated by very recent overprints. A second component appears above 10 mT in AF demagnetization and usually decays linearly to the origin (Figure 3a, with almost no low coercivity overprint; Figure 3c; Figure 3g with a large low-coercivity overprint, with reverse polarity compared to the second component). About 40% of the NRM are removed by 20 mT, and 80% is removed by 80 mT. Figure 3e shows a case where (at least) two components largely overlap in AF. Thermal demagnetization is often similar to and consistent with AF demagnetization (Figures 3c and 3d). The higher-temperature component is sometimes very linear (Figures 3b and 3d) and sometimes more noisy (Figures 3f and 3h). Figure 3f shows that TH demagnetization is in some cases more efficient to separate two components than AF, whereas Figure 3h shows a medium temperature overprint extending up to 350°C. The direction of the more robust component appears consistent but better determined by AF in that case. The evolution of selected demagnetization curves (Figure 4) confirms that medium destructive fields and median unblocking temperatures are of the order of 20 to 50 mT and 300 to 550°C, respectively, with some exceptions (e.g., in Figure 3a, sample GA1303b is still not half demagnetized at 100 mT; on the contrary, in Figure 4, sample GA2105 has lost 60% of its magnetization by 5 mT). Demagnetization is most often complete by 580°-600°C. In a few cases, a small component with the same direction persists up to 620°C. These and a large database of earlier results on stratoid basalts [see *Manighetti*, 1993] confirm that (titano-) magnetites with high unblocking temperatures (close to the Curie temperature of magnetite) are the dominant carriers of the characteristic remanent magnetization (ChRM) of the samples.

4. Paleomagnetic Directions

In most cases, determination of ChRM was rather straightforward, and the directions were identified using both the AF and TH methods, whenever they could be clearly identified in twin specimens. However, before introducing and discussing these results, it is interesting to report some more detailed observations.

4.1. Comparing Instruments and Demagnetization Techniques

Figure 5a shows the mean directions (ChRM) obtained respectively for (1) samples measured and AF-demagnetized with the 2G magnetometer, (2) samples AF-demagnetized with the Schönstedt apparatus and then measured with the JR5 magnetometer, and (3) samples thermally demagnetized and then measured with the JR5. The three means (with declination and inclination equal to 9.1°±2.1°, -9.1°±2.1°; 7.4°±2.9°, -

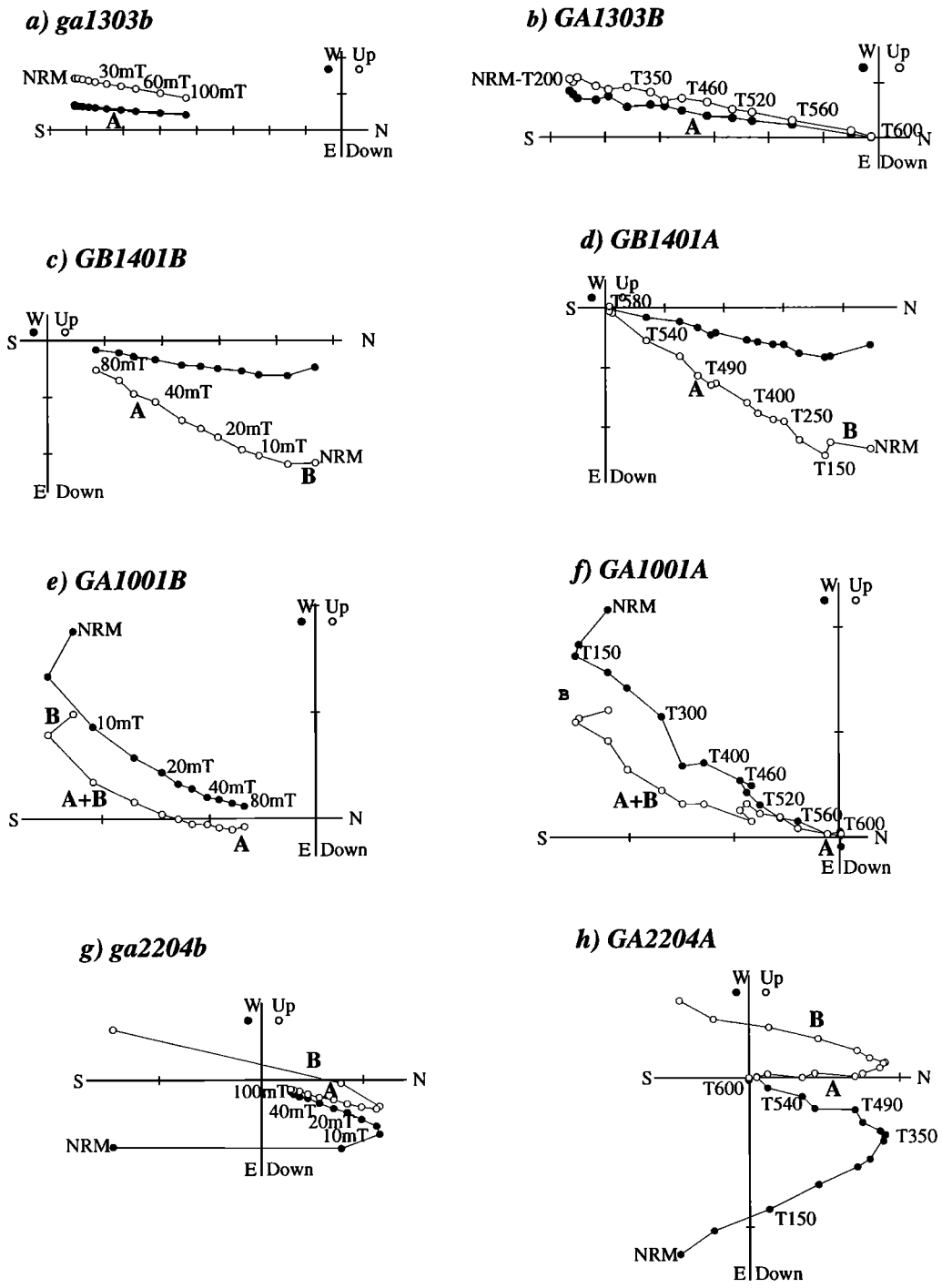

Figure 3. Vector demagnetization diagrams for typical specimens: (left) alternating field (AF) demagnetization (field in mT) and (right) thermal demagnetization (temperatures in °C). Specimens shown on the same line are from the same core. See text for discussion. Solid circles are for the component in the horizontal (N-S versus W-E) plane; open circles are for the component in the N-S vertical plane. The scale is 1 A/m per segment in all diagrams. Primary and secondary components (A and B) are indicated.

8.1°±2.9°; and 6.7°±3.2°, -10.7°±3.1°, respectively) have overlapping 95% confidence intervals, between 2° and 3°, and are not mutually distinguishable, confirming both that the two magnetometers yield identical results (to instrument uncertainty at least) and that the two demagnetization techniques also do. All results could therefore be merged in the following calculations.

4.2. Comparing Flows Offset by a Small Fault

Although such a fault could be identified in the field and the corresponding flows tentatively matched, evidence was far from certain. Figure 5b shows that the mean ChRMs clearly confirm (or at least are consistent with) the fact that GB11 and GA21 on one hand and GB12 and GA22 on the other hand show

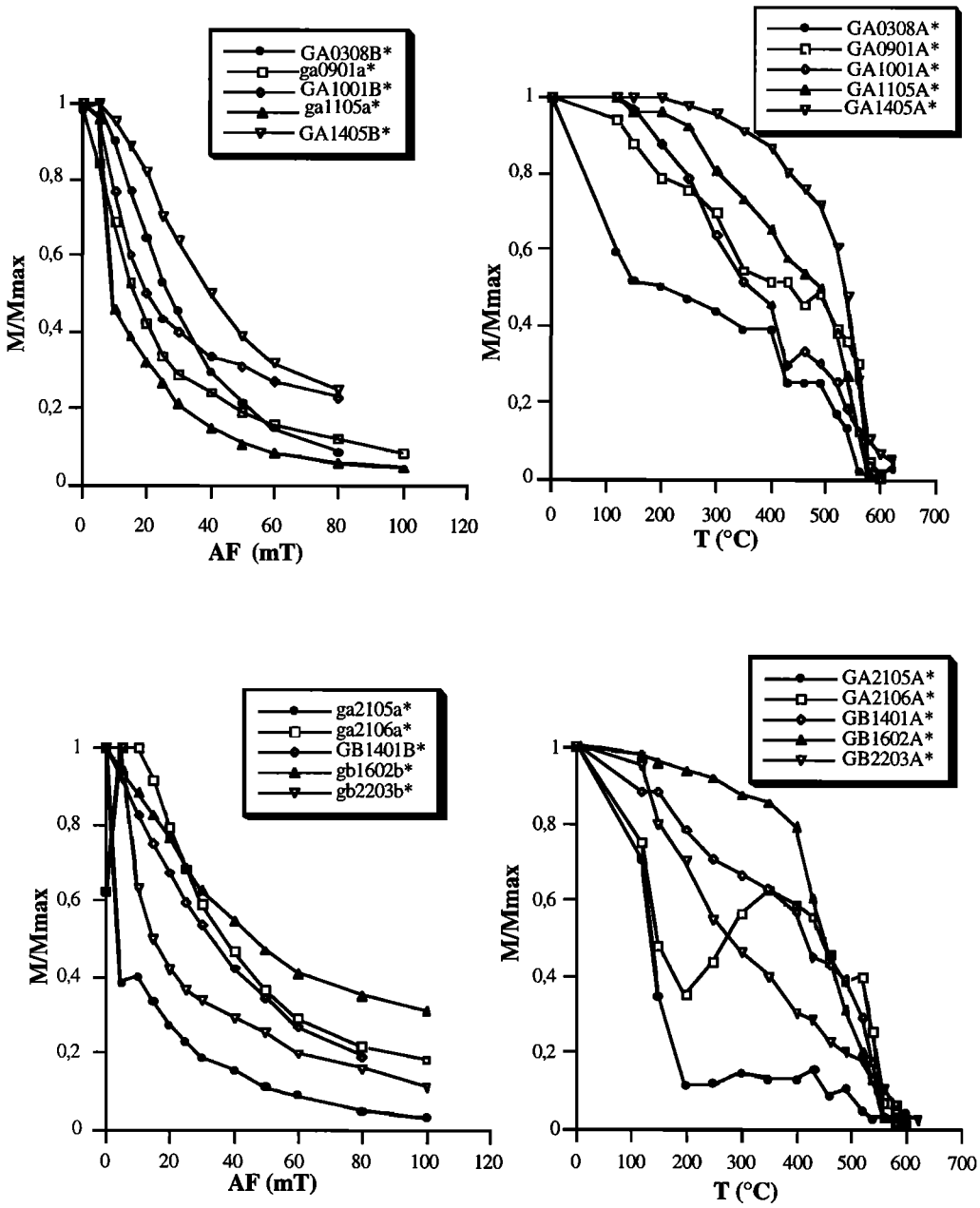

Figure 4. Normalized intensity curves for AF and thermal demagnetization (M/Mmax versus field or temperature), showing representative behavior of several samples.

the same mean directions and hence come from the same flows. The fact that these are two sequences of two successive flows, with the same succession of quite different directions, is particularly strong evidence in this respect. This is a nice paleomagnetic test of an in-the-field geological hypothesis and allows us to merge the two sequences of flows into a single continuous one. Directions from GB11 and GA21 (GB12 and GA22, respectively) will be averaged to provide the mean for each of these flows.

4.3. Specimens With Different TH and AF Results

In two cases, specimens behaved in a very different way and yielded apparently contradicting results using the two techniques. Figure 6 shows that AF demagnetization of GA0901a reveals two components of magnetization with a large overlap. The low-coercivity component has approximately normal polarity with low inclination; the high-coercivity one tends to be reversed with low inclination. Remagnetization circles [*Halls*, 1976, 1978] show that the poorly separated higher-coercivity component indeed has reversed polarity and is compatible with the directions found from other samples from the same flow. On the other hand, TH demagnetization would seem to yield a low-temperature component (LTC) up to 100°C, then a single component up to the Curie temperature of magnetite. The demagnetization pattern is noisy, with a zigzag pattern between 400° and 500°C. The normalized demagnetization curve shows significant unblocking at 300°-350°C. In any case, the TH behavior, which yields a meaningless direction, must result from complete overlap of two components and does not allow isolation of an

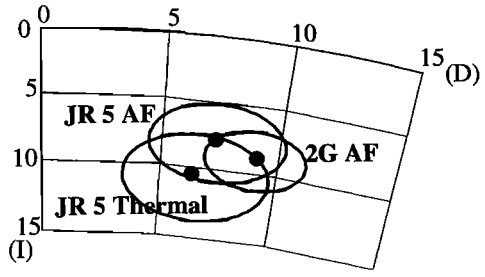

Figure 5a. Stereographic projection showing the characteristic mean directions and confidence intervals obtained for different sets of measurements: 2G AF, measured and AF demagnetized with 2G cryogenic magnetometer (163 specimens); JR5 AF, measured with JR5 magnetometer and AF demagnetized (92 specimens); JR5 Thermal, measured with JR5 magnetometer and TH demagnetized (120 specimens).

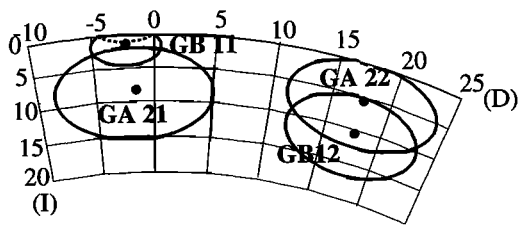

Figure 5b. Stereographic projection of the characteristic mean directions and confidence intervals from four sites located on two sides of a normal fault in the Gamarri section. Sites GA21 and GA22 are on the upper part of the downfaulted block, while sites GB11 and GB12 are on the lower part of the upfaulted block.

interpretable ChRM. A case with opposite behavior (artifact AF, trustable TH) was also encountered. This underlines the importance of systematically analyzing twin specimens by both methods whenever possible.

4.4. A very unusual flow

Figure 7 shows a series of AF and TH demagnetization diagrams for flow GB19. This flow is particularly interesting since the underlying one is close to normal polarity and the one above is fully reversed. Hence there was hope to catch a transitional direction. TH demagnetization shows from one to possibly four discrete straight-line segments. On closer inspection, many samples display a low temperature component C up to about 300°C, then sometimes an intermediate component C? (possibly resulting from overlap of two components) between 400° and 430°-460°C, a higher unblocking temperature component B up to 540°C, then the highest unblocking temperature component A up to the Curie temperature GB1901B and GB1905B display the sequence C - C? - B - A, GB1904A displays the sequence B – A, and GB1906A displays the sequence C - B. AF demagnetization is unable to resolve these components and shows complex S-shaped curves, with different coercivity sequences (Figure 8: e.g., GB1901B, GB1905B). Separation is apparently better in GB1904c, although the order of components is C - A - B. GB1903A shows only a low-coercivity component, then B.

This set of measurements would seem to support the existence of three magnetization components: C and C? with low coercivity and low unblocking temperatures, B with medium temperatures (430-540°C) and a complex coercivity spectrum, with both low and higher coercivities, and, finally, A with higher temperatures (540°-580°C, but also possibly unblocking in the 300°-450°C range) and medium coercivities. This pattern suggested several hypotheses, one with A as the primary magnetization and B as a later significant remagnetization. This is supported by the observation that the mean GB19 A component is quite close to the mean direction of

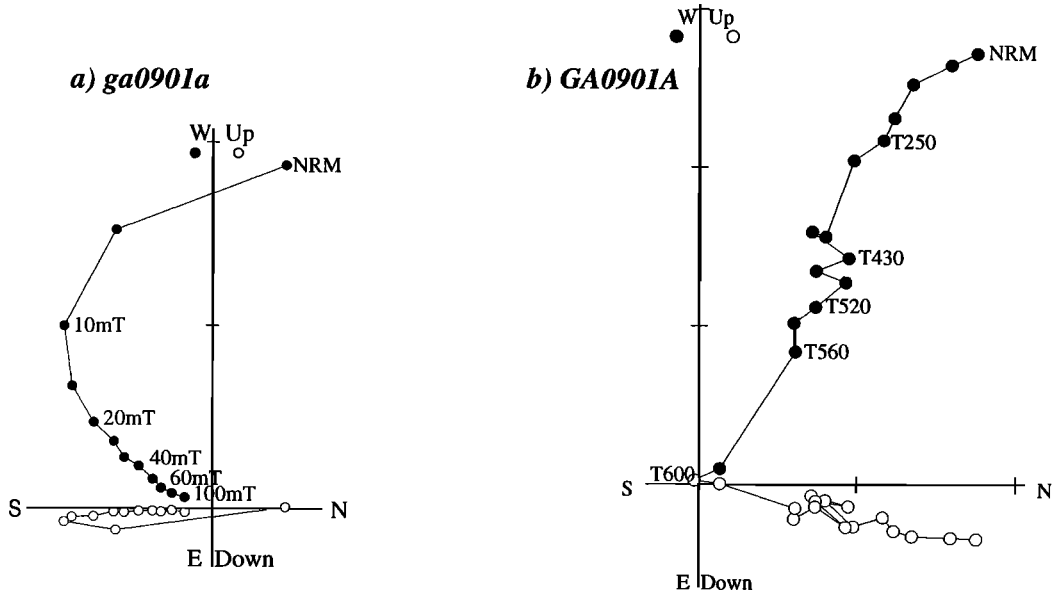

Figure 6. Vector component diagrams and AF and thermal demagnetization curves for twin specimens from the same core, for which thermal demagnetization fails to uncover overlapping components (see legend of Figure 3).

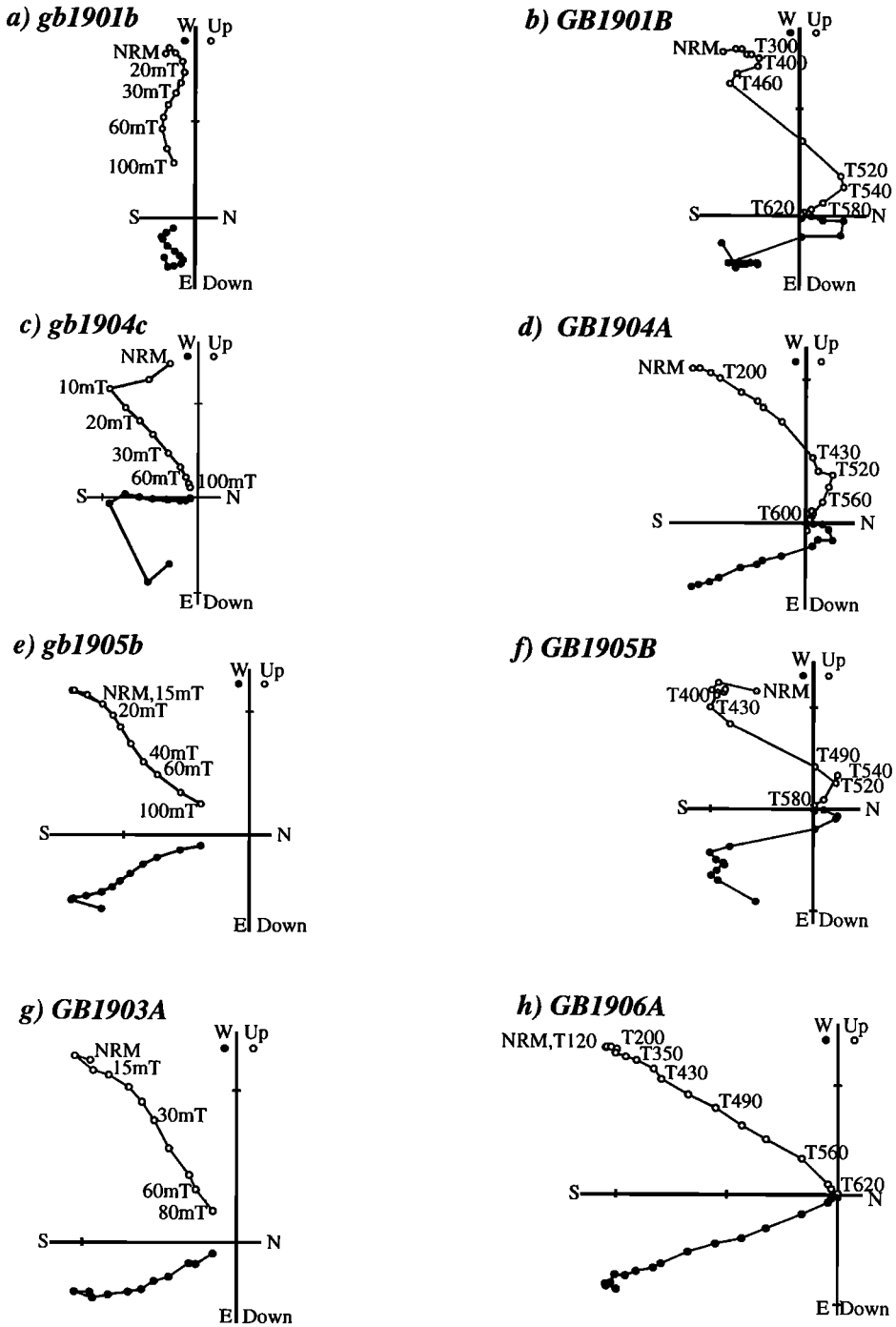

Figure 7. Same as Figure 3, but for four pairs of specimens from site GB19. See text for discussion.

the underlying flow GB18, whereas both the higher-coercivity and medium-temperature determinations of the B component are very close to the mean direction of the overlying flow GB20 (Figure 8). Moreover, all these mean directions lie close to a common great circle.

This behavior was fascinating enough that a new sampling trip was undertaken in 1997 to resample flow 19 in detail, taking careful notice of the position of the sample between the bottom and top of the 2 m thick flow. Also, the same kind of behavior was encountered by *Valet et al.* [1999] in supposedly transitional flows from the Brunhes-Matuyama reversal boundary in La Palma (Canary Islands). Detailed analyses of the La Palma and new Gamarri samples are the subject of a separate paper [*Valet et al.*, 1998]. This work confirms the idea that component A is likely to be the primary component of flow GB19, with transitional direction though close to that of GB18, and B a medium-temperature, probably thermochemical remagnetization acquired shortly after, at the time of emplacement of overlying flow GB20. This specific behavior could be revealed by TH demagnetization because of the conjunction of very low field intensity, baking by overlying flows, and the presence of a large amount of cation deficient

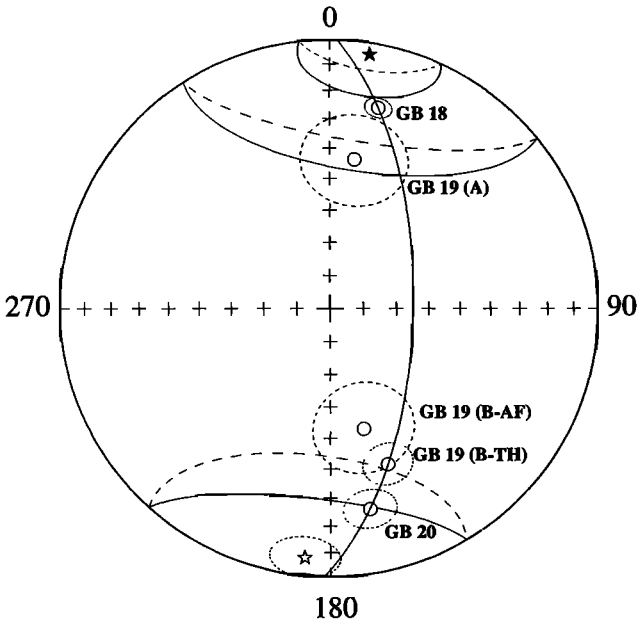

Figure 8. Different components of magnetization obtained from demagnetization of site GB19 and comparison of these directions with those from lava flows above (GB20) and below (GB18). The overall means for the normal and reversed polarity periods (star symbols) are also plotted with their respective 95% confidence intervals. GB19 components are A (high temperature), B-AF (medium coercivity), and B-TH (medium temperature); see text.

titanomagnetite [*Valet et al.*, 1998]. This would not have been easy to spot for a flow sandwiched between two other flows, all with the same polarity.

4.5. Mean Flow Directions

With the above comments in mind, mean directions have been calculated for all 33 successive independent flows from the Gamarri section. They are listed (with relevant parameters) in Table 1 and are displayed, together with their 95% confidence intervals, in Figure 9. There are two groups of site mean directions with opposite polarities, with some intermediate directions (Figure 9). Using the recursive method proposed by *Vandamme* [1994] in order to evaluate the cutoff angle, six sites can indeed be considered as either transitional or excursional. When these sites are removed, the means of the normal and reversed sites taken separately are antipodal [*McFadden and McElhinny*, 1990]. They can therefore be combined to produce an overall mean for the Gamarri section. After tilt correction this direction is D=8.1°, I=10.1°, α_{95}=4.1° (K=47.8, N=27; Table 1).

Three "anomalous" directions (GA06-GA08) are found in the lower part of the sequence, which may correspond to a period of strong secular variation. When these three directions are included in calculation of the mean direction, the result is indistinguishable from the previous one (Table 1).

4.6. Magnetic Stratigraphy

Figure 10 shows the magnetic polarity sequence, together with the declination, inclination, and resulting virtual geomagnetic pole (VGP) latitude stratigraphies. The sequence is very simple. It outlines a normal interval consisting of seven flows, sandwiched between reversed flows (16 below, four above). As noted above, an episode of large inclination variation in the bottom third of the sequence (GA06, GA07, and GA08) might indicate transitional behavior, large-scale secular variation, or an aborted excursion. Three other lava flows have possibly intermediate directions, at the onset (GA20) and termination (GB18 and GB19) of the normal polarity interval (note that in Figure 10 directions have been corrected for tectonic rotation as discussed below).

5. Geochronology

The Afar stratoid series was originally dated to be between 0.4 and 4.4 Ma in age, using the conventional K-Ar technique [*Varet and Gasse*, 1978]. Using both updated K-Ar and ^{40}Ar-^{39}Ar, *Courtillot et al.* [1984] reduced this range to 1.3-2.2 Ma, at least in much of Djiboutian Afar. Several other K-Ar determinations, using the Cassignol-Gillot technique, were performed by one of us (Gillot) in the frame of the work by *Manighetti* [1993] [see also *Manighetti et al.*, 1997]. These tend to confirm the results of *Courtillot et al.* [1984], indicating that the 1500-m thick, trap-like stratoid series may have erupted as a rather catastrophic event (geologically speaking) in no more than 1 Myr, about 2 Myr ago. Six flows were carefully sampled in the Gamarri cliff (GA02, GA10, GA17, GA22, GB23, and GB30) for K/Ar dating in the Université de Paris Sud (UPS)-IPGP geochronology laboratory at Orsay. The Cassignol technique [*Cassignol and Gillot*, 1982] was used because it is based on a scale-like zero comparison of atmospheric argon, allowing accurate dating of lavas which are either very young and/or have low radiogenic content [*Gillot and Cornette*, 1986]; the sample preparation procedure and laboratory analysis are as described in the above papers. Freshness of the samples and lack of any mineralogical phases indicating possible alteration were first checked from thin section examinations. Samples were crushed and the 250-400 μm size fraction was retained in order to remove phenocrysts. After ultrasonic cleaning in 20% nitric acid solution for 1 hour, followed by careful rinsing and drying, early crystallized phases (plagioclase, olivine, and pyroxene phenocrysts) were eliminated using heavy liquids in order to reduce as much as possible the potential influence of inherited Ar. The remaining microlithic groundmass was used for both K and Ar measurements. Potassium was measured by atomic emission photometry and argon was measured with a mass spectrometer identical to that described by *Gillot and Cornette* [1986]. Calibration of the Ar signal to better than 1% uncertainty was achieved using replicate measurements of the interlaboratory calibrated standard GL-O [*Odin*, 1982], with the recommended value of 6.679 10^{-14} at $^{40}Ar^*$ g^{-1}. Uncertainties on K determinations are typically 1%, whereas those on Ar are a function of the radiogenic content of the sample.

All sampled lavas from the Gamarri section were indeed aphyric, except for GA17 with a strikingly distinct doleritic texture. Thin section examination suggested the presence of inherited plagioclase xenocrysts. The apparent age measured for this flow turned out to be about 10% older than all the other ones. This was therefore discarded and is not considered further. Results are given in Table 2 and shown in Figure 11, with a 1σ uncertainty. Mean values range from 2.02 to 2.14 Ma, or 1.95 to 2.20 Ma when the 1σ uncertainties are included. Mean values

Table 1. Site (Flow) Mean Directions After AF and TH Demagnetization for All Sites of the Gamarri Section

Site	N	D_g	I_g	D_s	I_s	k	α_{95}
GA01	6	189.0	-12.0	188.8	-7.1	174.9	5.1
GA02	8	189.6	-7.5	189.5	-2.5	202.0	3.9
GA03	7	190.7	-10.1	190.5	-5.1	81.8	6.7
GA04	8	206.0	-19.7	205.3	-15.2	72.7	6.5
GA05	8	197.7	-18.3	197.2	-13.5	113.4	5.2
GA06	7	183.5	34.2	183.7	39.2	31.2	11.5
GA07	9	175.2	39.8	174.9	44.8	106.5	5.0
GA08	8	168.5	-50.2	169.6	-45.3	288.0	3.3
GA09	9	189.5	-3.1	189.5	1.9	367.7	2.7
GA10	8	194.1	0.2	194.1	5.1	53.4	7.7
GA11	8	189.9	6.1	190.1	11.0	211.1	3.9
GA12	8	184.0	-2.4	184.0	2.6	70.2	6.7
GA13	8	186.1	-17.9	185.9	-12.9	608.0	2.2
GA14	8	186.6	-18.6	186.4	-13.6	411.8	2.7
GA15	8	188.1	-13.5	187.9	-8.6	464.4	2.6
GA16	10	187.5	-17.6	187.3	-12.7	323.4	2.7
GA17	8	187.7	-17.6	187.5	-12.6	223.8	3.7
GA18	8	182.8	-16.8	182.7	-11.8	77.7	6.3
GA19	8	186.0	-21.3	185.8	-16.3	175.2	4.2
GA20	8	154.5	-46.3	156.5	-41.8	441.7	2.6
GA21/GB11	14	357.9	9.8	358.0	4.8	138.5	3.4
GA22/GB12	14	17.6	13.9	17.3	9.1	102.2	4.0
GB13	6	357.5	21.8	357.6	16.8	44.0	10.2
GB14	6	11.1	26.6	10.6	21.7	121.5	6.1
GB15	6	8.5	11.0	8.4	6.1	265.7	4.1
GB16	6	14.4	18.7	14.1	13.9	117.2	6.2
GB17	7	13.4	38.5	12.6	33.6	202.6	4.3
GB18	6	13.3	-19.4	13.7	-24.2	377.6	3.5
GB19	4	8. 7	-38.2	9.4	-43.2	38.3	15
GB20	6	168.4	-29.6	168.9	-24.7	95.9	6.9
GB21	9	188.0	-17.9	187.8	-13.0	150.3	4.4
GB22	5	195.7	-14.9	195.4	-10.1	76.5	8.8
GB23	8	174.6	-10.4	174.6	-5.4	27.2	10.8
MEAN1	30	7.8	9.9	7.7	5.0	14.4	7.2
MEAN2	27	8.3	15.1	8.1	10.1	47.8	4.1

Sites GA21 and GB11 on one hand and GA22 and GB12 on the other hand, which belong to the same flows, have been averaged (see text). Table column headings: Site, site code number; N, number of samples; D_g and I_g, declination and inclination in geographic coordinates; D_s and I_s, declination and inclination in stratigraphic coordinates; K, Fisher precision parameter; α_{95}, 95% confidence interval.

are found not to be in strict stratigraphic order (GB30). A few phenocrysts were observed in lava GB30, which might have partly escaped separation by heavy liquids. These might have been incorporated by the lava at extrusion time or have crystallized in the magma chamber under high fluid pressure. Given uncertainties, all ages are consistent with the overall mean value of 2.07 ± 0.05 Ma. This is fully compatible with all earlier results on the stratoid series. The uncertainties (see Table 3 and Figure 11) are relatively large, reflecting the significant atmospheric contamination of these lavas.

6. Discussion

6.1. Tectonic Rotation

The Gamarri section is located in the southern part of the overlap zone defined by the Asal-Manda Inakir rifts to the north and the Manda Hararo rift to the south [*Manighetti*, 1993]. Much of this overlap zone has suffered rotations of the order of 10°, as first found by *Courtillot et al.* [1984] and confirmed by extensive further work [*Manighetti*, 1993]. If one

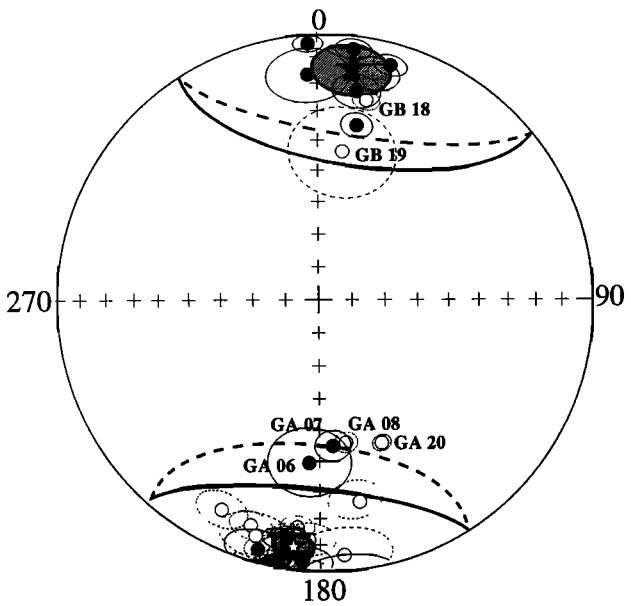

Figure 9. Stereographic projection showing all site means (circles) with α_{95} confidence intervals for all sites in the Gamarri section. Overall means for the reversed and normal data (with possibly transitional sites removed) are shown as star symbols (all symbols solid for lower hemisphere and open for upper hemisphere). Also shown in bold are the circles centered on the overall means with a radius equal to the standard deviation σ, suggesting possible transitional directions (flow number indicated).

follows the subdivision of the overlap zone into parallel strips [*Tapponnier et al.*, 1990], the Gamarri cliff forms the southwestern edge of a large block, the Gamarri-Dakka block. This block was found to have rotated clockwise by 11.1°±8.7° since the lavas covering it were extruded. For our Gamarri "super site" (given the number of sampled flows compared to that in individual sites used in other studies in Afar), a clockwise rotation of 8.1° ± 4.2° is found. The two values (Figure 12) are within the joint intersection of their 95% confidence intervals, a "class A" result (angular difference of 3.0°± 9.6°, indistinguishable from zero with high probability). The declination of the Gamarri section shows a difference of 7.2° ± 4.9° with respect to that of the average dipole field in Africa estimated for the last 2.0 Myr [*Besse and Courtillot*, 1991], and inclinations are not compatible (difference 12.1° ± 4.7°). This incompatibility in inclination has been repeatedly encountered within the Afar stratoid lavas [*Courtillot et al.*, 1984; *Manighetti*, 1993]. Moreover, a mean inclination of 7° and declination of 359° have been reported in sediments of the same age in the Hadar region, not far to the southwest [*Endale et al.*, 1996] and in the Omo region, southwest of Ethiopia [*Brown et al.*, 1978]. These sediments would seem to vindicate the " anomalous " Afar inclinations.

6.2. Secular Variation

Given the tectonic rotation suffered by the Gamarri-Dakka block, and by our Gamarri section along with it, one can correct observed mean directions for this rotation (Table 3). Corresponding VGPs can be calculated; their scatter is found to be 9.9° (confidence interval 8.3°-12.3°) when the six " transitional " directions are discarded [*Cox*, 1969]. When all 30 sites are considered, VGP scatter increases to 12.1° (confidence interval 10.3°-14.7°). Because two reversals are observed in the sequence and a total duration of the order of 10^5 years is indicated by the K/Ar ages, serial correlation is not expected, and the scatter of directions (or VGPs) should reflect paleosecular variation (PSV). The value we find when 30 sites are retained is compatible with the recent 0-5 Ma PSV model of *McFadden et al.* [1991] (Figure 13). However, the VGP scatter

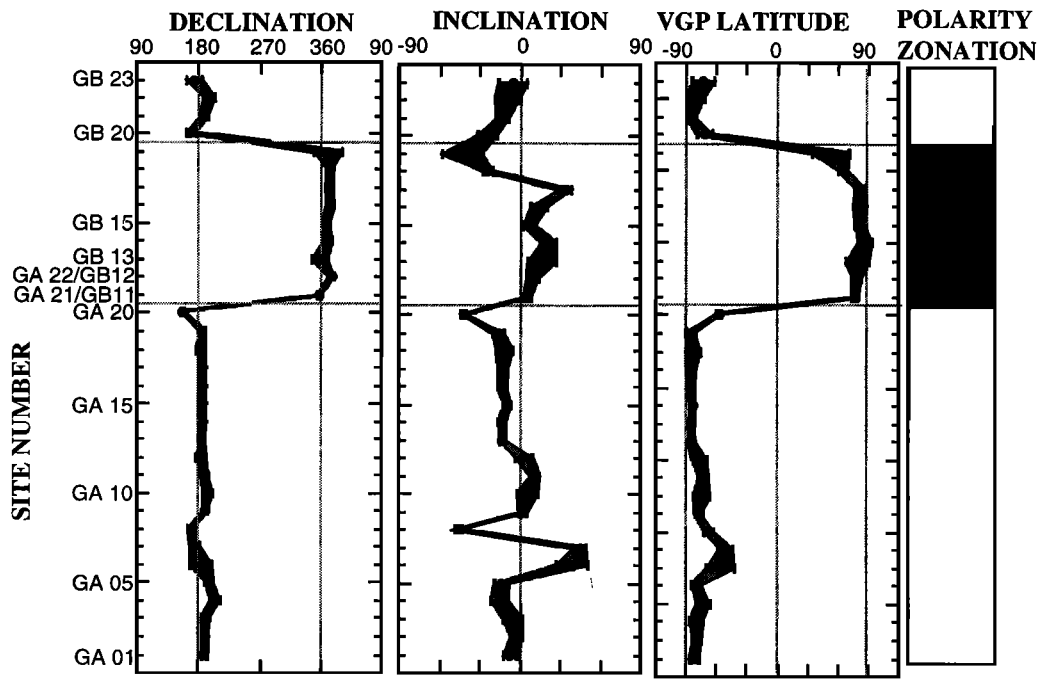

Figure 10. Magnetostratigraphy of the Gamarri section. Declinations, inclinations, and virtual geomagnetic pole (VGP) latitudes (after correction for tectonic rotation; see text), with their polarity zonations, are reported for all sites from base to top of section.

Table 2. Results of K-Ar Dating of Five Basaltic Lava Flows at Gamarri Section

Sample	K	Weight	$^{40}Ar^{*}$(%)	$^{40}Ar^{*}$(at)	Age	Uncertainty
GB30	1.026	1.00024	4.92	2.255	2.10	0.07
		2.01789	7.62	2.194	2.07	0.05
Mean (n=2)					(2.08)	(0.06)
GB23	0.832	1.50456	13.27	1.788	2.06	0.04
		1.50251	11.86	1.706	1.99	0.04
Mean (n=2)					(2.02)	(0.04)
GA22	0.525	1.01393	4.22	1.14	2.08	0.08
		1.00383	4.53	1.076	1.98	0.07
Mean (n=2)					(2.03)	(0.08)
GA10	0.783	1.00018	5.53	1.652	2.04	0.06
		0.9999	5.44	1.721	2.13	0.07
Mean (n=2)					(2.09)	(0.06)
GA2	0.355	1.80082	5.89	0.794	2.14	0.06
		1.00064	5.24	0.8	2.18	0.07
		2.00266	6.38	0.77	2.10	0.06
Mean (n=3)					(2.14)	(0.06)
Overall mean (N=5)					2.07	0.05

Table column headings: Sample, identification; K, total percentage of potassium in sample; Weight, weight of sample used for argon measurements (in grams); $^{40}Ar^{*}$(%), percentage of radiogenic argon 40 in sample; $^{40}Ar^{*}$(at),number of atoms of radiogenic argon 40 per gram of sample (in 10^{12} at/g); Age, age from replicate argon measurements for each sample in Ma (means of these replicate determinations are given in parentheses); uncertainity is at the 1 σ level. Decay constants of *Steiger and Jäger* [1977] have been used.

Table 3. Mean Directions and Poles From Gamarri Section and Reference Directions for Africa at 2.0 Ma

Means	N	D	I	K	α_{95}	ϕ	λ	A_{95}
Gamarri, unrotated								
Normal sites		8.3	15.2	41.5	9.5	156.2	81.0	9.7
Reversed sites	20	199.0	-8.31	52.4	4.6	354.1	-79.1	4.6
All sites	27	8.1	10.1	47.8	4.1	170.2	79.7	4.1
All selected sites, plus three «anomalous» sites (see text)	30	7.7	5.0	14.4	7.2	181.3	78.1	7.2
Gamarri, rotated								
Normal sites	7	0.2	15.2	41.5	9.5	219.1	86.1	9.7
Reversed sites	20	179.9	-8.3	52.4	4.6	42.2	-82.6	4.6
All sites	27	0.0	10.1	47.8	4.1	221.8	83.5	4.1
All selected sites, plus three «anomalous» sites (see text)	30	0.0	5.0	14.4	7.2	221.9	80.9	7.2
Reference directions and poles								
Besse and Courtillot [1991]	-	0.9	22.2	-	2.3	136.1	89.1	2.4
Manighetti [1993]	20	11.1	11.9	15.8	8..5	157.7	77.7	8.6

The first subset of results is for raw (unrotated) paleomagnetic results derived from Table 1. The second subset is corrected for tectonic rotation (see text). The third subset gives some reference directions and poles for Africa. Table column headings : N, number of flows, sites, or studies ; D and I, declination and inclination ; K and α_{95}, statistical parameters as in Table 1 ; ϕ and λ, and A_{95}, longitude, latitude, and 95% confidence interval of corresponding geomagnetic pole.

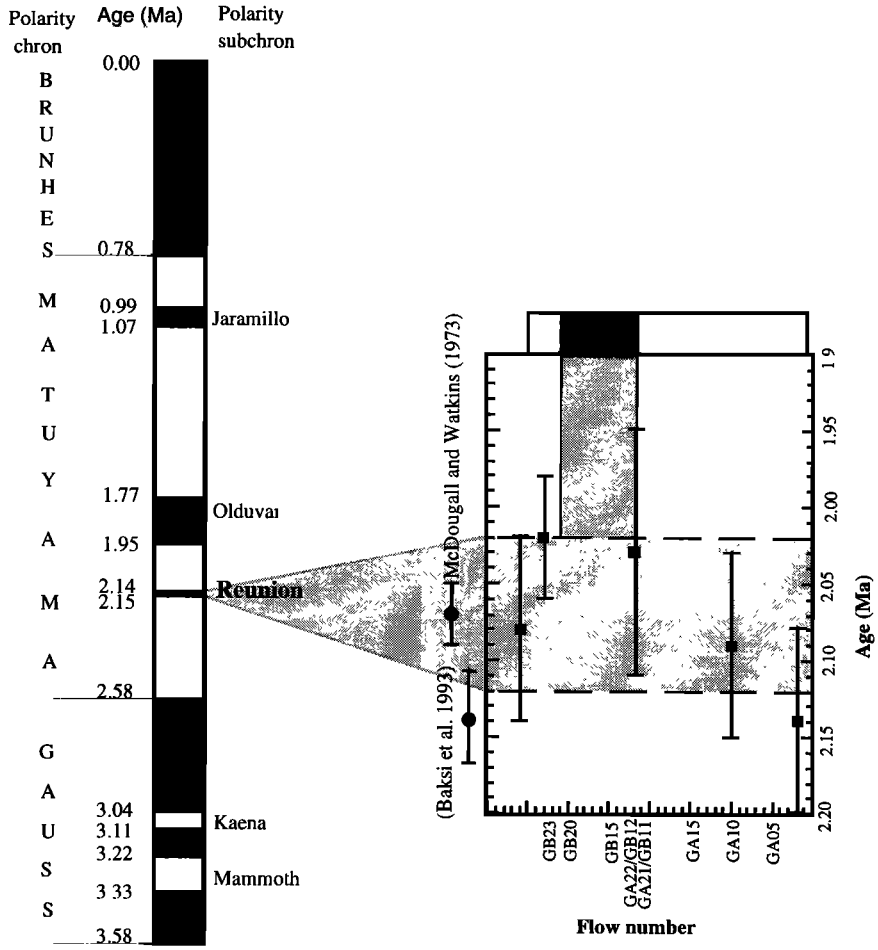

Figure 11. (right) K/Ar age determinations for five sites, with 1σ uncertainities, as a function of stratigraphy (see Table 3). Ages determined for the Réunion subchron by *McDougall and Watkins* [1973] and *Baksi et al.* [1993] are also given. (left) Correlation of the Gamarri section with the geomagnetic polarity timescale of *Cande and Kent* [1995].

value computed from 27 sites is significantly smaller than indicated by the model (which might indicate that secular variation was not sampled properly, although the mean direction remains similar). Such a difference illustrates the sensitivity of the VGP scatter estimate.

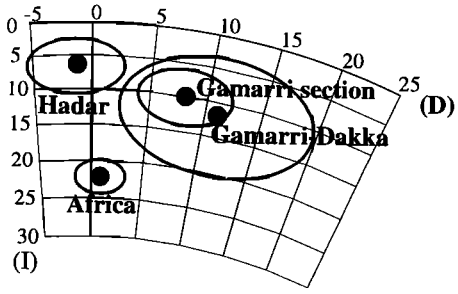

Figure 12. Stereographic projection showing overall mean direction for the Gamarri section and, for comparison, that obtained in the Gamarri-Dakka block farther east by *Manighetti* [1993]. Directions of the mean dipole field at 2 Ma for Africa [*Besse and Courtillot*, 1991] and overall mean direction for Hadar sediments [*Endale et al.*, 1996] are shown for comparison.

6.3. PSV Modeling

The above results underline two important points regarding the construction and use of PSV databases in order to derive information on the long-term structure of the mean geomagnetic field. First, we see that tectonic rotation precludes use of Afar data for such studies. The corrected values are model-dependent and hence should only be used with great caution (when, for instance, independent geological estimates of vertical axis rotation become available, which is not yet the case, but see *Manighetti* [1993]). Erroneous use of such data (i.e., failure to recognize the existence of tectonic deformation) in a small database would induce spurious nondipolar terms in long-term average field models [*Carlut and Courtillot*, 1998]. Second, we have seen that accurate directions for PSV studies require detailed full AF and TH demagnetization. A number of artifacts, which are not necessarily easy to spot, could arise: erroneous apparent ChRM in either AF-only or TH-only data, and unnoticed thermochemical remagnetizations, such as that found in GB19.

6.4. Magnetostratigraphy: The Réunion Subchron

The age and pattern of the R-N-R Gamarri sequence can be matched to a recent geomagnetic polarity timescale for

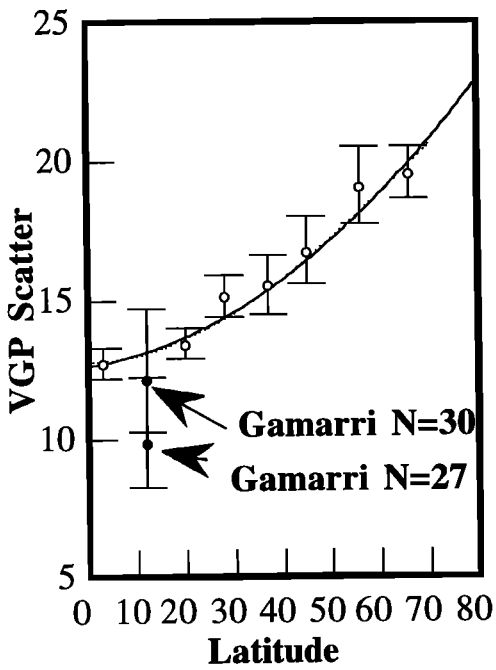

Figure 13. Comparison of VGP scatter determined for the Gamarri section (all sites, N=30; selected sites, N=27; see text) with the reference curve of *McFadden et al.* [1991] for the period 0-5 Ma.

tentative identification of chrons [e.g., *Cande and Kent*, 1995]. The Gamarri N interval cannot be correlated either with the Olduvai subchron or with the last normal subchron of the Gauss chron. The first case would imply that the ages of the upper Gamarri reversed flows are in error by at least 0.28 Ma, and the second one would imply that the ages of the lower Gamarri flows are in error by 1 Ma. It appears that only one correlation is possible, that is, with the Réunion subchron (Figure 11). This feature was first identified in Réunion Island (Indian Ocean) by *Chamalaun and McDougall* [1966] and *McDougall and Chamalaun* [1966]. The K/Ar age obtained by *McDougall and Watkins* [1973], when corrected for the more recent decay constants recommended by *Steiger and Jäger* [1977], is 2.07 ± 0.02 Ma, remarkably consistent with the value of 2.07 ± 0.05 Ma that we find. On the other hand, this is not compatible at the 1σ level (only at the 2σ level) with the more recent age of 2.14 ± 0.03 Ma proposed by *Baksi et al.* [1993]. The latter age was obtained by $^{40}Ar/^{39}Ar$ heating steps for whole rock samples drilled from the same flows dated by *McDougall and Watkins* [1973]. Because of the apparently high-precision dating of *Baksi et al.* [1993], the most recent geomagnetic polarity timescales [*Cande and Kent*, 1995] use values of 2.15 and 2.14 Ma for the upper and lower limits, respectively, of the subchron.

Two possibilities can be considered. The first is that the same geomagnetic feature is observed in Réunion and in Afar. Although the K/Ar and Ar/Ar techniques seem to indicate a different age at the 1σ level, some arguments may be put forward to reconcile these two ages. *Baksi et al.* [1993] explained the apparent discrepancy between results obtained by both techniques in terms of partial loss of radiogenic ^{40}Ar. However, the uncertainties calculated for each of the plateau ages by *Baksi et al.* [1993] seem to be underestimated. When standard methods (calculation of error associated to a weighted mean [*Taylor*, 1982]) are used to calculate uncertainties for the degassing steps selected by *Baksi et al.* [1993], the ages found for the lower transition are 2.15±0.09 and 2.15±0.12 Ma (flows RSD-43 and RSD-44, respectively), and the ages found for the upper transition are 2.15±0.03 and 2.08±0.07 Ma (flows RSD-53 and RSD-54, respectively). It can be noticed that uncertainties are significantly larger than the published values [*Baksi et al.*, 1993]. This could illustrate the limitations of whole-rock $^{40}Ar/^{39}Ar$ step-heating analyses and the way associated uncertainties are estimated. Furthermore, with these recalculated uncertainties, individual K/Ar [*McDougall and Watkins*, 1973] and $^{40}Ar/^{39}Ar$ ages [*Baksi et al.*, 1993] can be reconciled within a 1 σ uncertainty, except for only one flow (RSD-53), thereby casting some doubt on the conclusions of the latter authors regarding systematic differences between K/Ar and $^{40}Ar/^{39}Ar$ ages.

A second possibility is to consider that two distinct geomagnetic events occurred slightly before the Olduvai subchron. Recent paleomagnetic studies derived from continuous sedimentary sections indicate that minima in relative intensity variations can be used as indicators for the localization of the succession of excursions or very short subchrons [*Valet and Meynadier*, 1993]. In addition, when an independent timescale such as the astronomical timescale is available, the paleointensity curve can be used to determine a precise age for geomagnetic features. From the Ocean Drilling Program (ODP) leg 138 record, *Valet and Meynadier* [1993] identified a pronounced intensity minimum at 2.13 Ma, which they associated with the Réunion event, in agreement with the age obtained by *Baksi et al.* [1993]. However, another significant minimum is found at 2.03 Ma [*Valet and Meynadier*, 1993], which would be consistent both with the 2.07 ± 0.05 Ma mean we obtain and with our best determined individual age of 2.02 ± 0.04 Ma from flow GB23, shortly postdating the normal subchron. We might therefore have sampled not the Réunion event but a slightly younger geomagnetic feature. We may also propose that the earlier period of apparently strong secular variation which we find in the lower part of the Gamarri section (Figure 10) could represent an incomplete record of the geomagnetic event first identified at Réunion Island [*McDougall and Watkins*, 1973]. The age values determined for flows GA02 (2.09±0.06) and GA10 (2.14±0.06) (Table 2) would be consistent with this idea. However, because no densely sampled sedimentary section which could confirm the presence of several events exists within the time interval of concern here, this hypothesis remains highly tentative.

Uncertainties in isotopic ages do not allow us to robustly determine the total duration of the lava sequence. The ranges of values and 1σ uncertainties suggest a duration of the order of 100 kyr, with an average of one flow every 3 kyr (with very large uncertainties because of the irregular time sequence expected for volcanism). This would indicate a duration of the order of 30 kyr for the Réunion subchron itself. Given uncertainties, this cannot be distinguished from the 10 kyr duration which is usually suggested (10-50 kyr for *McDougall and Watkins* [1973]; 10 kyr for *Cande and Kent*, [1995]). The rather unique record of a very short geomagnetic feature in Gamarri, and the possibility of collecting further samples from other sections given the concentration of ages of the Afar stratoid series around 2 Ma, carry great promise for paleointensity studies and for testing the fine structure of the Réunion event. In particular, ongoing paleointensity

determinations on the Gamarri samples indicate that both the normal chron and the period of large secular variation in the preceding reverse chron likely correspond to low paleointensities [*Carlut et al.*, 1997].

7. Conclusion

The remarkable set of quasi linear, high cliffs generated by normal faulting in the active floor of the Afar depression provides unique opportunities to sample long, fresh sequences of young basaltic lavas that were deposited as flat, thick, trap-like flows over a vast expanse. The most voluminous and pervasive formation is the stratoid series (at least 1.5 km thick), with ages apparently ranging from 1.3 to 2.2 Ma, with a rather significant pulse around 2 Ma. Extensive paleomagnetic sampling in space has provided evidence for a pattern of organized block rotations [*Courtillot et al.*, 1984; *Manighetti*, 1993], interpreted in terms of propagating and overlapping rift zones. Further results from a series of 33 successive flows, collected along the Gamarri cliff and reported in this paper, confirm the ~10° clockwise rotation of the Gamarri-Dakka block, one of the strips of crust undergoing bookshelf faulting as described by *Tapponnier et al.* [1990]. More interestingly from a geomagnetic point of view, the new sequence displays a series of three polarities. Directions have recorded a short normal polarity interval. K/Ar dating at 2.07±0.05 Ma implies high extrusion rates (one flow per few thousand years, with a large uncertainty) and allows the identification of this interval with the Réunion subchron or a slightly younger event. The age is compatible with that first proposed by *McDougall and Watkins* [1973] but is less so with the more recent GPTS of *Cande and Kent* [1995]. It is the only detailed recording of this very short subchron by volcanic flows outside of the locus typicus in Réunion. Moreover, considering "anomalous" directions observed in the lower part of the Gamarri section, it is possible that this section has recorded the fine double structure of the Réunion event which has sometimes been reported.

Exceptional extrusion rates, large lava volumes, widespread exposure, and very limited alteration in the Afar depression make this region an outstanding location for further detailed work not only on the Réunion subchron, but possibly also on Olduvai and, more generally, on patterns of paleosecular variation in much of the dominantly reversed Matuyama chron.

Acknowledgments. We thank V. Bachtadse, L. Tauxe, and an anonymous referee for useful comments on the manuscript. This is IPGP contribution 1583.

References

Baksi, A. K., A. K. Hoffman, and M. McWilliams, Testing the accuracy of the geomagnetic polarity time-scale (GPTS) at 2-5 Ma, utilizing $^{40}Ar/^{39}Ar$ incremental heating data on whole-rock basalts, *Earth Planet. Sci. Lett.*, **118**, 135-144, 1993.

Besse, J., and V. Courtillot, Revised and synthetic apparent polar wander paths of the African, Eurasian, North American and Indian plates, and true polar wander since 200 Ma, *J. Geophys. Res.*, **96**, 4029-4050, 1991.

Brown, F.H., R.T. Shuey, and M.K. Croes, Magnetostratigraphy of the Shungura and Usno Formations, southwestern Ethiopia: New data and comprehensive reanalysis, *Geophys. J. R. Astron. Soc.*, **54**, 519-538, 1978.

Cande, S. C., and D. V. Kent, Revised calibration of the geomagnetic polarity timescale for the Late Cretaceous and Cenozoic, *J. Geophys. Res.*, **100**, 6093-6095, 1995.

Carlut, J., J.-P. Valet, Y. Gallet, T. Kidane, V. Courtillot, X. Quidelleur, and P.-Y. Gillot, Preliminary paleointensity results during the Reunion event (abstract), *IAGA, Abstract book, Uppsala, Sweden*, p 45, 1997.

Carlut, J., and V. Courtillot, How complex is the time averaged geomagnetic field over the last five million years?, *Geophys. J. Int.*, **134**, 527-544, 1998.

Cassignol, C, and P.-Y. Gillot, Range and effectiveness of unspiked potassium-argon dating in *Numerical Dating in Stratigraphy*, edited by G.S. Odin, pp. 159-172, John Wiley, New York, 1982.

Chamalaun, F. H., and I. McDougall, Dating geomagnetic polarity epochs in Réunion, *Nature*, **210**, 1212, 1966.

Courtillot, V., Opening of the Gulf of Aden and Afar by progressive tearing, *Phys. Earth Planet. Inter.*, **21**, 343-350, 1980.

Courtillot, V., Propagating rifts and continental breakup, *Tectonics*, **1**, 239-250, 1982.

Courtillot, V., J. Achache, F. Landre, N. Bonhommet, R. Montigny, and G. Féraud, Episodic spreading and rift propagation: New paleomagnetic and geochronologic data from the Afar nascent passive margin, *J. Geophys. Res.*, **89**, 3315-3333, 1984.

Cox, A., Confidence limits for the precision parameter K, *Geophys. J. R. Astron. Soc.*, **18**, 545-549, 1969.

Endale, T., N. Thouveny, and M. Taieb, Magnetostratigraphy of the Hadar Formation (Ethiopia): evidence for a short normal event in the Mammoth subchron, *Stud. Geophys. Geod.*, **40**, 313-336, 1996.

Fischer, R. A., Dispersion on a sphere, *Proc., R. Soc. London, Ser. A.*, **217**, 295-305, 1953.

Gillot, P.-Y., and Y. Cornette, The Cassignol technique for potassium-argon dating, precision and accuracy: Examples from the late Pleistocene to recent volcanics from southern Italy, *Chem. Geol.*, **59**, 205-222, 1986.

Gruszow, S., Etude aéromagnétique et paléomagnétique du territoire de la République de Djibouti, Ph.D. thesis, 211 pp., Univ. Paris 7, 1992.

Halls, H. C., A least-squares method to find a remanence direction from converging remagnetization circles, *Geophys. J. R. Astron. Soc.*, **45**, 297-304, 1976.

Halls, H. C., The use of converging remagnetization circles in paleomagnetism, *Phys. Earth Planet. Inter.*, **16**, 1-11, 1978.

Johnson, C. L., and C. G. Constable, The time-averaged geomagnetic field as recorded by lava flows over the past 5 Myr, *Geophys. J. Int.*, **122**, 489-519, 1995.

Johnson, C. L, and C. G. Constable, Paleosecular variation recorded by lava flows over the past five million years, *Philos. Trans. R. Soc. London, Ser. A.*, **354**, 89-141, 1996.

Kirschvink, J. L., The least squares line and plane and the analysis of paleomagnetic data, *Geophys. J. R. Astron. Soc.*, **62**, 699-718, 1980.

Manighetti, I., Dynamique des systèmes extensifs en Afar, Ph.D. thesis, 242 pp., Univ. Paris 6, 1993.

Manighetti, I., P. Tapponnier, V. Courtillot, S. Gruszow, and P.-Y. Gillot, Propagation of rifting along the Arabia-Somalia plate boundary: The gulfs of Aden and Tadjoura, *J. Geophys. Res.*, **102**, 2681-2710, 1997.

McDougall, I., and F. H. Chamalaun, Geomagnetic polarity scale of time, *Nature*, **212**, 1415, 1966.

McDougall, I., and N. D. Watkins, Age and duration of the Réunion geomagnetic polarity event, *Earth Planet. Sci. Lett.*, **19**, 443-452, 1973.

McElhinny, M.W., P.L. McFadden, and R. T. Merrill, The time-averaged paleomagnetic field 0-5 Ma, *J. Geophys. Res.*, **101**, 25,007- 25,027, 1996.

McFadden, P.L., and M.W. McElhinny, The combined analysis of remagnetization circles and direct observations in paleomagnetism, *Earth Planet. Sci. Lett.*, **87**, 152-160, 1988.

McFadden, P.L., and M.W. McElhinny, Classification of the reversal test in paleomagnetism, *Geophys. J. Int.*, **103**, 725-729, 1990.

McFadden, P. L., R.T. Merrill, and M. W. McElhinny, Dipole/quadrupole family modeling of paleosecular variation, *J. Geophys. Res.*, **93**, 11,583-11,588, 1988.

McFadden, P. L., R.T. Merrill, M.W. McElhinny, and S. Lee, Reversals of the Earth's magnetic field and temporal variations of the dynamo families, *J. Geophys. Res.*, **96**, 3923-3933, 1991.

Odin, G.S. (Ed.), *Numerical Dating in Stratigraphy*, 2 vol., 1094 pp., John Wiley, New York, 1982.

Prévot, M., and S. Grommé, Intensity of magnetization of subaerial and sub-marine basalts and its possible change with time, *Geophys. J. R. Astron. Soc.*, **40**, 207-224, 1975.

Quidelleur, X., and V. Courtillot, On low-degree spherical harmonic models of paleosecular variation, *Phys. Earth Planet. Inter.*, **95**, 55-77, 1996.

Quidelleur, X., J.-P. Valet, V. Courtillot and G. Hulot, Long-term geometry of the geomagnetic field for the last five million years: An updated secular variation database, *Geophys. Res. Lett.*, **21**, 1639-1642, 1994.

Steiger, R. H., and E. Jäger, Subcommission on geochronology: Convention on the use of decay constants in geo- and cosmochronology, *Earth Planet. Sci. Lett.*, **36**, 359-362, 1977.

Tapponnier, P., R. Armijo, I. Manighetti, and V. Courtillot, Bookshelf faulting and horizontal block rotation between overlapping rifts in southern Afar, *Geophys. Res. Lett.*, **17**, 1-4, 1990.

Taylor, J.R., An introduction of error analysis, 270 pp., Univ. Sci. Books, Mill Valley, Calif., 1982.

Valet, J. -P., and L. Meynadier, Geomagnetic field intensity and reversals during the past four million years, *Nature*, **366**, 234-238, 1993.

Valet, J.-P., T. Kidane, V. Soler, J. Brassart, V. Courtillot, and L. Meynadier, Remagnetization in lava flows recording pretransitional directions, *J. Geophys. Res.*, **103**, 9755-9775, 1998.

Valet, J.-P., J. Brassard, X. Quidelleur, V. Soler, P.-Y. Gillot, and L. Hongre, Paleointensity variations across the last geomagnetic reversal at La Palma, Canary Islands, Spain, *J. Geophys. Res.*, in press, 1999.

Vandamme, D., A new method to determine paleosecular variations, *Phys. Earth. Planet. Inter.*, **85**, 131-142, 1994.

Varet, J., Geological Map of central and southern Afar (Ethiopia and F.T.A.I), 1:500 000; Beicip, France, 1975.

Varet, J., and F. Gasse, Geology of central and southern Afar (Ethiopia and Djibouti Republic), *Centre National de la Recherche Scientifique*, Paris, 1978.

J. Carlut, V. Courtillot, Y. Gallet, T. Kidane, and X. Quidelleur, Laboratoire de Paléomagnétisme et Géodynamique, Institut de Physique du Globe de Paris, 4, Place Jussieu, Tour 24-14 1er etage, 75252 Paris Cedex 05, France. (courtil@ipgp.jussieu.fr)

P.Y. Gillot, Laboratoire de Géochronologie, Université Paris Sud, Institut de Physique du Globe de Paris, Bât 504, 91405 Orsay, France.

T. Haile, Department of Geology and Geophysics, Addis Ababa University, P.O. Box 1176, Addis Ababa, Ethiopia.

(Received July 21, 1998; revised December 28, 1998; accepted January 6, 1999.)